Polariton Condensation in Photonic Molecules

Marta Galbiati,[1] Lydie Ferrier,[1] Dmitry D. Solnyshkov,[2] Dimitrii Tanese,[1] Esther Wertz,[1] Alberto Amo,[1] Marco Abbarchi,[1] Pascale Senellart,[1] Isabelle Sagnes,[1] Aristide Lemaître,[1] Elisabeth Galopin,[1] Guillaume Malpuech,[2] and Jacqueline Bloch[1,*]

[1]*CNRS-Laboratoire de Photonique et Nanostructures, Route de Nozay, 91460 Marcoussis, France*
[2]*LASMEA, CNRS, Clermont University, University Blaise Pascal, 24 avenue des Landais, 63177 Aubière cedex, France*
(Received 1 July 2011; revised manuscript received 17 January 2012; published 20 March 2012)

We report on polariton condensation in photonic molecules formed by two coupled micropillars. We show that the condensation process is strongly affected by the interaction with the cloud of uncondensed excitons and thus strongly depends on the exact localization of these excitons within the molecule. Under symmetric excitation conditions, condensation is triggered on both binding and antibinding polariton states of the molecule. On the opposite, when the excitonic cloud is injected in one of the two pillars, condensation on a metastable state is observed and a total transfer of the condensate into one of the micropillars can be achieved. Our results highlight the crucial role played by relaxation kinetics in the condensation process.

DOI: 10.1103/PhysRevLett.108.126403 PACS numbers: 71.36.+c, 67.85.Hj, 78.55.Cr, 78.67.Pt

Most of the experimental studies in atomic Bose condensates have explored conditions of thermodynamic equilibrium, since typical condensate lifetimes are much longer than interaction times. Recent theoretical proposals have shown that out-of-equilibrium bosonic systems present qualitatively new behaviors [1]. One proposed way to reach this regime is the use of photonic systems with effective photon-photon interactions and dissipation provided by inherent optical losses [2]. Localized to delocalized phase transitions [3,4], highly entangled states [5], or fermionization effects in a ring of coupled sites [6] are predicted in such systems.

Microcavity polaritons are a model system for the investigation of the physics of driven-dissipative boson condensates [7–13]. They are the quasiparticles arising from the strong coupling between excitons confined in quantum wells and the optical mode of a microcavity. Because of their light-matter nature, polaritons present peculiar properties: They interact efficiently with their environment through their excitonic part [14,15], while their photonic part enables efficient coupling with the free space optical modes. Polariton condensates can be generated in zero-dimensional micropillars [11] or in arrays of pillars with fully controlled coupling [16,17]. In this configuration, the nonequilibrium nature of polariton condensates should allow the realization of metastable collective states, such as the self-trapped states in a bosonic Josephson junction [18–20].

In the present Letter, we investigate polariton condensation in photonic molecules obtained by coupling two micropillars. We demonstrate that polariton interactions strongly affect the way condensation occurs in such a coupled system, not only modifying the wave function of the polariton condensate but also the relaxation dynamics. This effect, specific to an out-of-equilibrium bosonic system, is illustrated by considering different positions of the nonresonant excitation within the molecule. When the excitation spot is placed at the center of the molecule, polariton condensation is observed on both binding and antibinding states. Interactions induce strong changes in the condensate wave function, the most important one being the change in its spatial anisotropy.

When the excitation spot is positioned on one of the two coupled micropillars, condensation occurs in a very different way. As the excitation power is increased, the polariton condensate is first created in a metastable state localized in the excited pillar by an effect similar to self-trapping [18]. By further increasing the pumping power, the condensation tends to progressively evolve from a kinetic regime to a regime closer to thermodynamical equilibrium: Massive occupation is observed on the lowest energy state of the system, mainly localized in the nonexcited pillar. These results are simulated by using a relaxation model including semiclassical Boltzmann equations and the nonlinear Schrödinger equation in a self-consistent way. The key features of our experiments can be reproduced only if one properly includes the changes of the relaxation rates due to interaction-induced modifications of the overlaps between the different polariton states.

The microcavity sample, described in Ref. [11], consists in a $\lambda/2$ cavity containing 12 GaAs quantum wells. Coupled micropillars were fabricated by using electron beam lithography and inductively coupled plasma dry etching. The diameter d of the micropillars ranges from 3 to 4 μm, and their center to center distance d_{CC} is varied from 2.3 to 3.7 μm, corresponding to an expected coupling constant between 0.1 and 1 meV. Note that d_{CC} is always kept smaller than twice the radius of the pillars, ensuring the direct coupling of the polariton modes of the two micropillars. A scanning electron micrography of an array

of such photonic molecules is shown in Fig. 1(a). Microphotoluminescence experiments are performed on single molecules by using a single mode cw Ti:sapphire laser focused onto a 2 μm diameter spot with a microscope objective. The sample is maintained at 10 K, and the excitation laser energy is tuned typically 100 meV above the lower polariton resonance, thus providing nonresonant optical excitation of the system. The emission is collected through the same objective and imaged on the entrance slit of a monochromator. The spectrally dispersed emission is detected with a nitrogen-cooled CCD camera. We define the detuning $\delta = E_c - E_x$ as the energy difference between the lowest energy photonic mode and the exciton resonance.

The polariton modes in these photonic molecules are investigated by photoluminescence measurements at low excitation power. An example of an emission spectrum measured on a single molecule is presented in Fig. 1(a). Discrete emission peaks are observed corresponding to polariton quantum states fully confined in the microstructure. The broader line at higher energy is due to emission of the excitonic reservoir. The two lowest energy modes (labeled B and A) are attributed to the binding and antibinding states arising from the hybridization of the lowest energy mode of each micropillar. The splitting between these states is proportional to the coupling between the two micropillars. It can be continuously tuned by changing the center to center distance d_{CC}, as illustrated in Fig. 1(b). The left column of Fig. 1(c) shows the spatial distribution (near field) of the four lowest energy modes in a molecule made of two 4 μm pillars with $d_{CC} = 3.73$ μm (the first two panels correspond to the B and A modes). The right column shows the calculated polariton wave functions considering a confinement potential taken as infinite outside the photonic molecule and equal to zero inside. As schematically illustrated in Fig. 1(d), all these states result from the hybridization of the optical modes of each individual micropillar, showing the strong analogy between our system and the orbitals of a diatomic molecule. We have spectrally measured a quality factor in the photonic molecule exceeding 16 000 (resolution limited). Time-resolved measurements (not shown here) indicate a polariton lifetime of the order of 35 $\pm$ 5 ps for zero detuning [21].

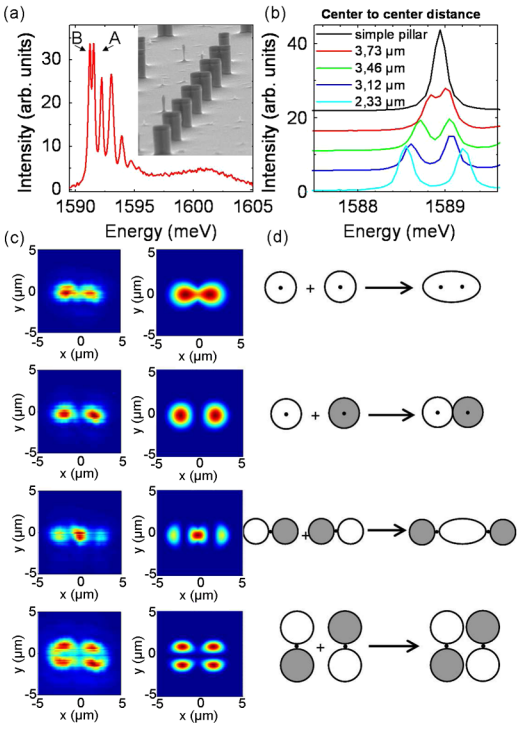

FIG. 1 (color online). (a) Emission spectrum measured on a single molecule at low excitation power ($d = 4$ μm and $d_{CC} = 3.73$ μm); A and B indicate the binding and antibinding states, respectively. Inset: Scanning electron micrograph of an array of pillars and molecules. (b) Emission spectra measured on a 4 μm round micropillar (black line) and on photonic molecules with $d = 4$ μm and various values of d_{CC}. (c) Left (right) column: Measured (calculated) emission pattern of the four lowest energy modes of a photonic molecule with $d = 4$ μm and $d_{CC} = 3.73$ μm. (d) Schematic of the hybridization of the individual pillar modes within a photonic molecule.

We now discuss polariton condensation in these molecules under nonresonant optical excitation. As we have shown in our recent work on single micropillars [22], such an excitation scheme not only populates the confined polariton states but also creates a population of uncondensed excitons called the excitonic reservoir. Because of the limited diffusion length of excitons, this reservoir remains localized in the excitation area. Repulsive interactions between polaritons and the excitonic reservoir strongly influence the precise quantum state in which polaritons accumulate. In the following, we will consider two different locations of the excitonic reservoir within the molecule, which can be selected via the position of the excitation laser spot. First we will consider excitation conditions where the reservoir of uncondensed excitons is at the center of the molecule. Then we will address the case of asymmetric excitation, in which the excitonic reservoir is injected only in one of the two micropillars. Specific spatial behavior of the polariton condensates is observed in each case, driven by the polariton interaction with the excitonic reservoir.

Figures 2(a)–2(c) present the measured emission distribution along the axis of a photonic molecule excited at its center. As summarized in Fig. 3(a), above a well-defined excitation threshold, a strong nonlinear increase of the emission intensity is observed, one of the signatures of polariton condensation [11]. Under this excitation condition, a massive accumulation of polaritons occurs in both the binding and antibinding lowest energy polariton states. Interestingly, as the excitation power is increased, a progressive change of the spatial shape of the polariton wave function is observed, with vanishing probability density at the center of the molecule. This behavior is

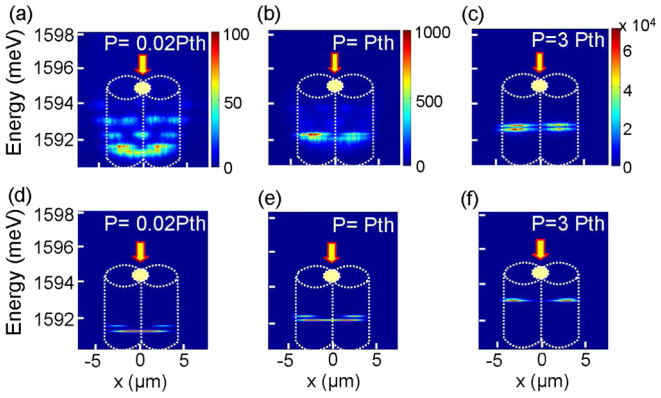

FIG. 2 (color online). Excitation at the center of the molecule: (a)–(c) spectrally resolved emission distribution along the molecule axis measured for several excitation powers; (d)–(f) calculated emission patterns for several excitation powers. $d = 4$ μm and $d_{CC} = 3.46$ μm. $\delta = -3$ meV.

due to repulsive interactions with the excitonic reservoir injected in that region.

To describe our experiments, we simulate polariton relaxation by using coupled semiclassical Boltzmann equations and nonlinear Schrödinger equations in a self-consistent way [23]. As described in the Supplemental Material, on one hand, a nonlinear Schrödinger equation is solved at each time iteration, in the presence of the potential induced by the excitonic reservoir and by the occupation of the polariton states, to find the eigenstates of the system. On the other hand, the time evolution of these occupation numbers is calculated by using the semiclassical Boltzmann equations in which the scattering rates are obtained by using the exact shape of the polariton states obtained from the nonlinear Schrödinger equation. Both exciton-phonon and exciton-exciton scattering mechanisms are considered. The reservoir is assumed to be thermalized at the lattice temperature. The key ingredient to describe our experiments is to consider scattering rates proportional to the spatial overlap between initial and final states. For instance, the scattering rate of two excitons from the reservoir resulting in one polariton in state i and one exciton in the reservoir is proportional to $\int |\psi_i(x,y)|^2[\rho_R(x,y)]^3 dxdy$, where $\psi_i(x,y)$ is the wave function of the polariton state i and $\rho_R(x,y)$ is the spatial distribution of the excitonic reservoir, described by a Gaussian of width w_R. To fit the data, we use an exciton-exciton scattering rate $W_{XX} = 2 \times 10^3$ s^{-1} and an exciton-phonon scattering rate $W_{XP} = 10^9$ s^{-1}. The lifetime of the reservoir is equal to 400 ps, and that of the polariton states to 30 ps (value for $\delta = -3$ meV).

The results of the model for central pumping are shown in Figs. 2(d)–2(f). The potential of the reservoir increases with the optical pumping and has a maximum at the center of the molecule, inducing the spatial separation of the states of each micropillar. As a result, both the coupling and the associated splitting between the two lowest energy states decrease. Indeed, this feature is shown in Fig. 3(b): Simultaneous to the spatial separation of the polariton distributions, the measured splitting goes down to a minimum at about $P = 4P_{th}$. At higher powers, the measured splitting tends to increase again. In the following, we will show that at such high density the observed splitting is no longer related to the binding-antibinding splitting but is an anisotropic splitting induced by the lateral spatial shrinking of the condensate wave function in each micropillar. This feature is not reproduced by our model, which does not include the polarization degree of freedom.

Polarization-resolved measurements were performed for different excitation densities. Figures 3(c) and 3(d) display emission spectra linearly polarized parallel and perpendicular to the molecule axis, below and above threshold. In the low density regime [Fig. 3(c)], the presence of uncondensed excitons has a negligible effect, and we observe a polarization splitting in both the binding and antibinding states. As previously reported theoretically and experimentally [24], this splitting is larger for the binding state and amounts to 70 μeV. The inset in Fig. 3(c) shows that the overall shape of the polariton binding state is elongated along the molecule. This is why the lowest energy line of the binding state doublet is polarized parallel to the molecule axis. The situation is different at high density ($P > 4P_{th}$), where a stronger potential barrier is induced by the excitonic reservoir at the center of the

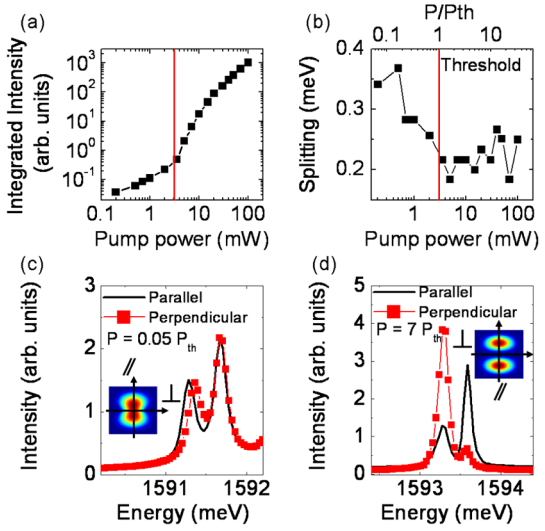

FIG. 3 (color online). Excitation at the center of the molecule: (a) integrated intensity measured as a function of the excitation power; (b) splitting between the two lowest energy emission lines measured as a function of the excitation power; (c) lowest energy emission lines measured with a polarization parallel (solid line) and perpendicular (squares) to the molecule axis for $P = 0.05P_{th}$; (d) the same as (c) for $P = 7P_{th}$. The inset shows the calculated spatial shape of the binding state.

molecule. In this case, the interpillar tunnel coupling becomes too small to be resolved in our experiment. The observed splitting comes from the anisotropic shape of the condensate in each pillar. Indeed, the polariton wave function is shrunk by the excitonic repulsive potential, and thus it is more elongated perpendicularly to the molecule axis. This change in anisotropy is evidenced in the polarization of the emission. The lowest energy emission line is now strongly polarized perpendicular to the molecule axis.

Different dynamics is observed when the laser spot is positioned on top of one of the micropillars forming the molecule. Emission distributions measured under these conditions are reported in Figs. 4(a)–4(c). Close to threshold, condensation occurs in the pillar that is optically pumped. Interparticle interactions blueshift the energy of the ground state in the pumped pillar, decoupling it from the states of the other pillar and severely limiting the Josephson transfer of particles from one pillar to the other. This localization is very analogous to the original self-trapping effect, except that here the blueshift is mainly induced by the interaction between the exciton reservoir and the condensate and not by interactions within the condensate itself. As the excitation power is increased, the better relaxation kinetic and the presence of excited states in the unpumped pillar destroy the metastable state [25] and allow the system to reach its ground state. Condensation then occurs in the nonpumped micropillar [Fig. 4(c)].

We can reproduce this overall behavior by using the self-consistent polariton relaxation model presented above. As shown in Fig. 4(d), at low power the reservoir potential creates an asymmetry in the two bottom states of the molecule, whereas the upper states are not affected. The populations of the excitonic states in the reservoir are small, and their relative distribution is given by the lattice temperature. When pumping increases [Fig. 4(e)], condensation starts at the eigenstate possessing the largest overlap integral with the reservoir. This corresponds to the third polariton state (population n_3). The reservoir potential also significantly perturbs the two bottom states, which become both confined in the right pillar. This blocks the direct relaxation from the reservoir towards these states and further enforces condensation in the third metastable state localized in the pumped pillar. At high pumping [Fig. 4(f)] a new effect is observed: Condensation is triggered onto the ground state (of population n_1). This does not arise from direct scattering from the reservoir, since the overlap between the ground state and the reservoir remains very small. This condensation is the result of efficient scattering from the intermediate third state toward the ground state via acoustic phonons. This regime occurs when the phonon-assisted scattering rate $W_{XP}n_3(1 + n_1)$ from the intermediate state into the ground state overcomes the ground state radiative losses $n_1\tau_1$. This happens when $n_3 \approx 100$, and further increase of the pumping does not change n_3 but only increases n_1. The second quantized state remains weakly populated: It has a smaller overlap with the reservoir than the third state and a higher energy than the ground state. Overall, the complete condensation dynamics can be understood only by considering the modifications of the relaxation rates induced by interactions (as shown in the Supplemental Material [23], when constant scattering rates are considered, condensation in the metastable states cannot be reproduced).

In conclusion, we have demonstrated polariton condensation in photonic molecules, a fully controlled system in which the coupling constant between two condensates can be adjusted. Depending on the precise location of the excitonic reservoir, strong renormalization of the polariton states is induced, resulting in strong modification of the condensation dynamics. In particular, condensation can occur in a metastable localized state or in the ground state of the system. These results open the way towards a detailed investigation of Josephson oscillations [26] or, more generally, the pumped-dissipative physics of arrays of coupled condensates in an engineered environment.

This work was supported by the C'Nano Ile de France (Sophiie2), by the ANR (PNANO-07-005 GEMINI and ANR-11-BS10-001), by the "Triangle de la Physique" (Picorre), by the FP7 ITN "Clermont4" (235114), and by the FP7 ITN "Spin-Optronics" (237252).

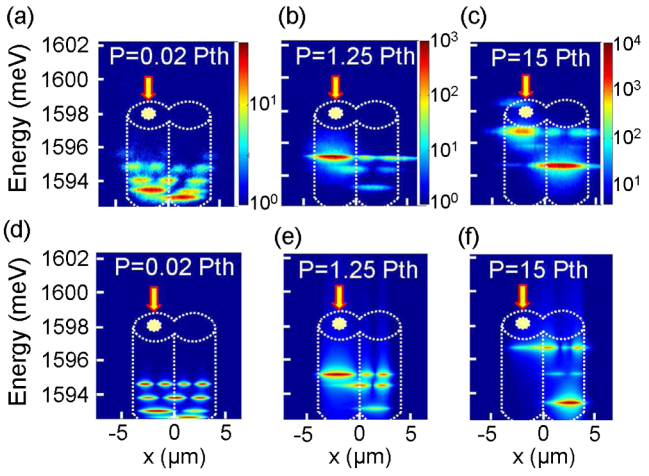

FIG. 4 (color online). Asymmetric excitation: (a)–(c) spectrally resolved emission distribution along the molecule axis measured for several excitation powers; (d)–(f) calculated emission patterns for several excitation powers. $d = 3.5\ \mu$m and $d_{CC} = 3.1\ \mu$m. $\delta = -3$ meV.

*jacqueline.bloch@lpn.cnrs.fr

[1] P. Werner, K. Volker, M. Troyer, and S. Chakravarty, Phys. Rev. Lett. **94**, 047201 (2005).
[2] D. Gerace *et al.*, Nature Phys. **5**, 281 (2009).
[3] A. D. Greentree *et al.*, Nature Phys. **2**, 856 (2006).

[4] S. Schmidt, D. Gerace, A. A. Houck, G. Blatter, and H. E. Türeci, Phys. Rev. B **82**, 100507(R) (2010).
[5] M. J. Hartmann *et al.*, Nature Phys. **2**, 849 (2006).
[6] I. Carusotto, D. Gerace, H. E. Tureci, S. De Liberato, C. Ciuti, and A. Imamolu, Phys. Rev. Lett. **103**, 033601 (2009).
[7] J. Kasprzak *et al.*, Nature (London) **443**, 409 (2006).
[8] R. Balili *et al.*, Science **316**, 1007 (2007).
[9] C. W. Lai *et al.*, Nature (London) **450**, 529 (2007).
[10] S. Christopoulos, G. Baldassarri Höger von Högersthal, A. J. D. Grundy, P. G. Lagoudakis, A. V. Kavokin, J. J. Baumberg, G. Christmann, R. Butté, E. Feltin, J.-F. Carlin, and N. Grandjean, Phys. Rev. Lett. **98**, 126405 (2007).
[11] D. Bajoni, P. Senellart, E. Wertz, I. Sagnes, A. Miard, A. Lemaître, and J. Bloch, Phys. Rev. Lett. **100**, 047401 (2008).
[12] E. Wertz *et al.*, Nature Phys. **6**, 860 (2010).
[13] E. A. Cerda-Méndez, D. N. Krizhanovskii, M. Wouters, R. Bradley, K. Biermann, K. Guda, R. Hey, P. V. Santos, D. Sarkar, and M. S. Skolnick, Phys. Rev. Lett. **105**, 116402 (2010)
[14] F. Tassone and Y. Yamamoto, Phys. Rev. B **59**, 10 830 (1999).
[15] C. Ciuti, P. Schwendimann, B. Deveaud, and A. Quattorpani, Phys. Rev. B **62**, R4825 (2000).
[16] M. Bayer, T. Gutbrod, J. P. Reithmaier, A. Forchel, T. L. Reinecke, P. A. Knipp, A. A. Dremin, and V. D. Kulakovskii, Phys. Rev. Lett. **81**, 2582 (1998).
[17] G. Guttroff, M. Bayer, A. Forchel, P. A. Knipp, and T. L. Reinecke, Phys. Rev. E **63**, 036611 (2001).
[18] A. Smerzi, S. Fantoni, S. Giovanazzi, and S. R. Shenoy, Phys. Rev. Lett. **79**, 4950 (1997).
[19] D. Sarchi, I. Carusotto, M. Wouters, and V. Savona, Phys. Rev. B **77**, 125324 (2008).
[20] I. A. Shelykh, D. D. Solnyshkov, G. Pavlovic, and G. Malpuech, Phys. Rev. B **78**, 041302 (2008).
[21] The quality of inductively coupled plasma dry etching, with respect to reactive ion etching, explains such a long lifetime as compared to Ref. [11].
[22] L. Ferrier, E. Wertz, R. Johne, D. D. Solnyshkov, P. Senellart, I. Sagnes, A. Lemaître, G. Malpuech, and J. Bloch, Phys. Rev. Lett. **106**, 126401 (2011).
[23] See Supplemental Material at http://link.aps.org/supplemental/10.1103/PhysRevLett.108.126403 for a description of the model used to calculate polariton relaxation.
[24] S. Michaelis de Vasconcellos *et al.*, Appl. Phys. Lett. **99**, 101103 (2011).
[25] M. T. Martinez, A. Posazhennikova, and J. Kroha, Phys. Rev. Lett. **103**, 105302 (2009).
[26] K. G. Lagoudakis, B. Pietka, M. Wouters, R. Andre, and B. Deveaud-Pledran, Phys. Rev. Lett. **105**, 120403 (2010).